Geomechanics and Engineering, *Vol. 29, No. 1 (2022) 79-90*
https://doi.org/10.12989/gae.2022.29.1.079

Biocementation via soybean-urease induced carbonate precipitation using carbide slag powder derived soluble calcium

Yongshuai Qi[a], Yufeng Gao*, Hao Meng[b], Jia He[c] and Yang Liu[d]

Key Laboratory of Ministry of Education for Geomechanics and Embankment Engineering, Hohai University, Nanjing 210098, China

(Received July 6, 2021, Revised December 5, 2021, Accepted December 21, 2021)

Abstract. Soybean-urease induced carbonate precipitation (EICP), as an alternative to microbially induced carbonate precipitation (MICP), was employed for soil improvement. Meanwhile, soluble calcium produced from industrial waste carbide slag powder (CSP) via the acid dissolution method was used for the EICP process. The ratio of CSP to the acetic acid solution was optimized to obtain a desirable calcium concentration with an appropriate pH. The calcium solution was then used for the sand columns test, and the engineering properties of the EICP-treated sand, including unconfined compressive strength, permeability, and calcium carbonate content, were evaluated. Results showed that the properties of the biocemented sand using the CSP derived calcium solution were comparable to those using the reagent grade $CaCl_2$. Scanning electron microscopy (SEM) and X-ray diffraction (XRD) analyses revealed that spherical vaterite crystals were mainly formed when the CSP-derived calcium solution was used. In contrast, spherical calcite crystals were primarily formed as the reagent grade $CaCl_2$ was used. This study highlighted that it was effective and sustainable to use soluble calcium produced from CSP for the EICP process.

Keywords: biocementation; carbide slag powder (CSP); soil improvement; soybean crude urease extract; soybean-urease induced carbonate precipitation (EICP)

1. Introduction

Microbially induced carbonate precipitation (MICP) as an innovative biocementation approach for soil improvement has been widely studied in recent years (Whiffin *et al.* 2007, Paassen *et al.* 2010, Chu *et al.* 2012, Cheng *et al.* 2013, Martinez *et al.* 2013, Qabany and Soga 2013, Sidik *et al.* 2014, Montoya and DeJong 2015, Al Imran *et al.* 2019, Choi *et al.* 2019, Do *et al.* 2019, Hang *et al.* 2019, Meng *et al.* 2021a). The biocementation process utilizes soluble calcium, urea, and ureolytic microorganisms or bacteria to precipitate calcium carbonate ($CaCO_3$) in situ to improve soil's physical and mechanical properties such as strength and compressibility. The biochemical process of MICP can be briefly described by the reactions

$$CO(NH_2)_2 + 2H_2O \xrightarrow{\text{ureolytic microorganisms or bacteria}} 2NH_4^+ + CO_3^{2-} \quad (1)$$

$$Ca^{2+} + CO_3^{2-} \rightarrow CaCO_3 \downarrow \quad (2)$$

In the process, ureolytic microorganisms or bacteria catalyzes the hydrolysis of urea to produce carbonate (CO_3^{2-}) and meanwhile brings out an increase in pH. In the presence of calcium ions, calcium carbonate ($CaCO_3$) that can fill tiny pores and bind loose particles is formed in the soil, resulting in an improvement of strength and a reduction of permeability.

However, the MICP-based biocementation has some challenges for soil improvement. For one thing, nutrients for ureolytic microorganisms or bacteria cultivation are expensive, and injecting ureolytic bacteria into the soil involves many issues, such as obtaining approvals and licenses from the government (Achal *et al.* 2010, Ran and Kawasaki 2016). For another, the MICP process usually requires a large amount of calcium chloride to produce adequate cementing calcium carbonate, the production of calcium chloride is energy-intensive and environmentally unfriendly (Chung *et al.* 2014). To address the first issue, urease extracted from bacteria and plant has been used for the biocementation process, known as enzyme induced carbonate precipitation (EICP) (Nam *et al.* 2014, Park *et al.* 2014, Hamdan and Kavazanjian 2016, Dilrukshi *et al.* 2018, Almajed *et al.* 2019, Gao *et al.* 2019, He *et al.* 2020, Hoang *et al.* 2019, Song *et al.* 2020, Meng *et al.* 2021b). For instance, Javadi *et al.* (2018) used a simple method of blending, filtration, and acetone fractionation to extract and purify urease from watermelon seeds for EICP treatment of soil. Tirkolaei *et al.* (2020) used a similar process to extract

*Corresponding author, Professor
E-mail: yfgao66@163.com
[a]Ph.D. Student
E-mail: qyslovelove@163.com
[b]Ph.D.
E-mail: hhumenghao@hotmail.com
[c]Associate Professor
E-mail: hejia@hhu.edu.cn
[d]Ph.D. Student
E-mail: land@hhu.edu.cn

ISSN: 2005-307X (Print), 2092-6219 (Online)

crude urease from jack beans, jack bean meal, soybeans, and watermelon seeds, and found that the crude urease is more effective than commercially available urease enzymes at enhancing soil strength. Cuccurullo *et al.* (2020) used two kinds of soybeans-derived urease (liquid soybeans extract and fine soybeans powder) to improve strength and durability of Bouisset soil via EICP. In contrast to the MICP method, the EICP method uses free urease instead of live microorganisms. Thus, it is free from issues that related to bio-safety and microbial growth (activity) control in soils (Ran and Kawasaki 2016, Khodadadi *et al*. 2017). Further, exogenously added urease (i.e. Urease added as a free enzyme) has a limited lifespan and its activity and function decrease with time. This limited lifespan is potentially advantageous in some engineering applications as the enzyme can naturally degrade and eliminate long term impacts to the ecosystem (Ran and Kawasaki 2016). To solve the second problem, researchers have taken many attempts to explore alternative calcium sources. For example, Cheng *et al.* (2014) proposed a new application of MICP technology in marine environments by using seawater as a source of calcium salt. Choi *et al.* (2016) adopted the soluble calcium that obtained by mixing eggshell with vinegar in the MICP process. Liu *et al.* (2018) used acetic acid to dissolve calcareous sand to gain calcium sources for biocementation. Choi *et al.* (2017a) developed a method to produce soluble calcium ions for the MICP process through two waste sources, limestone powder derived from aggregate quarries and acetic acid derived from fast pyrolysis of lignocellulosic biomass. Liang *et al.* (2019) used oyster shells, scallop shells, and eggshells to obtain calcium nitrate for MICP. Phua and Royne (2018) used calcium nitrate obtained from powdered limestone (chalk), and commercial urease enzyme derived from jack bean to biocement sands.

As a kind of alkaline industrial wastes, carbide slag is produced when PVC, PVA, acetylene, and other products are manufactured by the calcium carbide method. More than 40 million tons of carbide slags are produced worldwide each year (Tao *et al.* 2018). The recycling of carbide slag has aroused wide public concern (Junjie *et al.* 2014, Tao *et al.* 2018, Li *et al.* 2019, Wang *et al.* 2020)

In this work, crude urease extracted from soybean and soluble calcium produced from carbide slag powder (CSP) were employed for biocementation of sand via EICP. The extraction scheme was optimized to obtain a desirable calcium solution with an appropriate pH. A comparative study of EICP treatment using soluble calcium produced from CSP and reagent grade $CaCl_2$ with the same concentration of calcium was carried out. The physical and mechanical properties of the biocemented sand were evaluated through unconfined compressive strength (UCS) tests, permeability tests, scanning electron microscopy (SEM), and X-ray diffraction (XRD).

2. Materials and methods

2.1 Soybean-urease

Soybean (grown in Heilongjiang province, China) purchased from a nearby market was used to obtain the soybean-urease, and the process was as follows. A certain amount of air-dried soybean was crushed into powder by a kitchen grinder and passed through a 60-mesh sieve. The sieved soybean powder was added into deionized water at 40 g/L concentration, and the mixture was stirred for 20 minutes using a magnetic stirrer to obtain a homogeneous suspension. Then the suspension was centrifuged at 4,000 rpm and 20℃ for 15 minutes. After the centrifugation, the insoluble substances in the supernatant liquid were removed by filtering with a 200-mesh sieve. Finally, the supernatant liquid was collected as the soybean-urease solution without further purification. The soybean-urease solution prepared in this study had a urea-hydrolyzing activity of around 6.66 mmol/L/min.

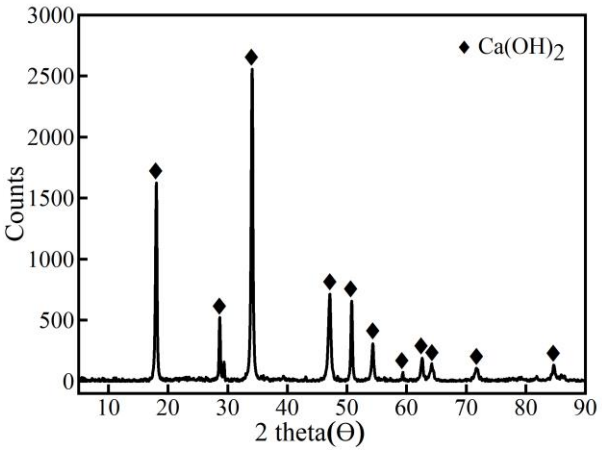

Fig. 1 The XRD pattern of carbide slag powder

2.2 Soluble calcium and cementation solution

In this paper, the soluble calcium solution was produced by dissolving CSP in the acetic acid solution. As a by-product of the acetylene plant, CSP was obtained from Yuanheng water purification material factory, Gongyi City, Henan Province, China. The CSP was dried at 105℃ for 24 hours to remove moisture for subsequent experiments. Chemical analysis of CSP using X-ray fluorescence spectroscopy (XRF) revealed that it contained 86.40% of calcium, 4.06% of sodium, 3.38% of silicon, 2.48% of Potassium, 1.14% of magnesium, 0.59% of fluorine,0.55% of sulfur, 0.45% of chlorine, 0.33% of aluminum, and 0.21% of iron. It can be inferred from the XRD pattern (Fig. 1) that the main composition of the CSP is calcium hydroxide ($Ca(OH)_2$). Acetic acid was used to dissolve the CSP, and the calcium ion is derived as follows

$$2CH_3COOH+Ca(OH)_2 \rightarrow 2(CH_3COO)^- +Ca^{2+}+2H_2O \quad (3)$$

To optimize the reaction conditions of CSP and acetic acid for calcium solution production, CSP was mixed with various concentrations of acetic acid solutions at different solid-to-liquid ratios (w/v). The pH and calcium concentrations of the aqueous solutions were determined by

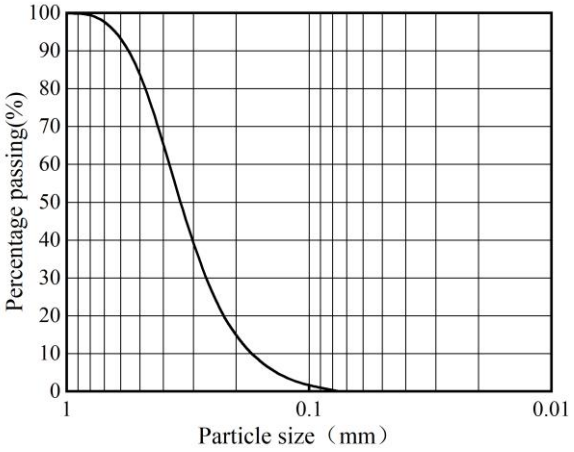

Fig. 2 Particle size distribution of ASTM graded Ottawa sand

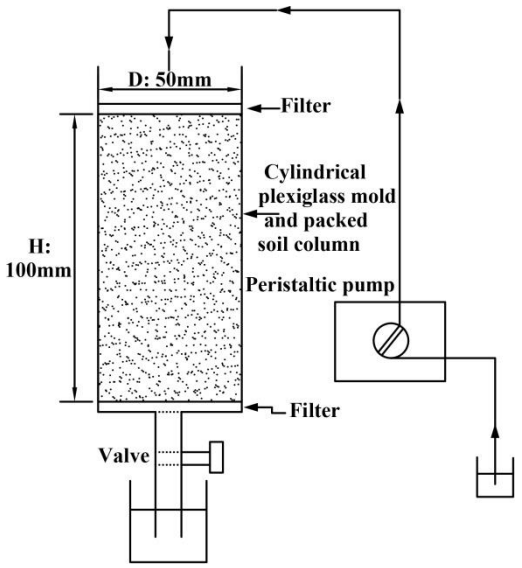

Fig. 3 Test setup schematic for EICP-based biocementation in the sand column

a pH meter and the EDTA titration method (Choi *et al.* 2017b), respectively. The dissolving efficiency was calculated by weighing the mass change of CSP before and after the acetic acid dissolution.

After the reaction conditions being optimized, the calcium solution was collected, and the pH was adjusted to 7.0-7.5 with 2 M NaOH solution. The solution was centrifuged at 4,000 rpm for 20 min to obtain the supernatant. After that, the supernatant was further added with distilled water to adjust the final calcium ion concentration to 0.5 M, which serves as the final soluble calcium solution in the following EICP process. Urea was dissolved into the soluble calcium solution to reach a concentration of 0.5 M. Finally, cementation solution (soluble calcium solution-based) was obtained, which is termed as SC hereafter. Besides, the conventional cementation solution containing 0.5 M urea and 0.5 M reagent grade $CaCl_2$ was also used in this work. It is referred to CC in the following sections.

2.3 EICP process in soil-free solution tests

To investigate the effect of different calcium sources (soluble calcium or reagent grade $CaCl_2$) on the EICP process, a series of soil-free solution tests were carried out in beakers. 80 mL soybean-urease solution (6.66 mmol/L/min) was mixed with 80 mL SC (0.5 M) or CC (0.5 M), the mixed solution was placed at room temperature (25±2°C) and stirred evenly for 24 h. Calcium ion concentration was measured using the EDTA titration method at regular intervals to characterize the consumption of calcium ions in the EICP process with time. Finally, the precipitated substances were collected by filtering and dried at 105°C for 1 day. The dried substances were then analyzed with XRD.

2.4 EICP-based biocementation in sand column tests

Sand column tests were also carried out to evaluate the effect of different calcium sources (soluble calcium or reagent grade $CaCl_2$) on EICP-based biocementation.

Ottawa sand (ASTM graded) was used in this study (ASTM 2012), which was classified as poorly graded quartz sand with a mean size of 0.36 mm. The maximum and minimum void ratios were 0.753 and 0.467, respectively. The particle size distribution is shown in Fig. 2.

Cylindrical plexiglass mold (50 mm in diameter and 120 mm in length) with an opening in the middle of the base was used to prepare sand column specimens of 50 mm in diameter and 100 mm in height (Fig. 3). A gauze (300 mesh) was placed in the bottom of the mold to prevent sand from leaking through the opening. Dry sand was placed into each mold in three layers to achieve a relative density of 40%. After the surface of the sand sample being leveled, a 300 mesh gauze was placed on top.

To proceed with the EICP process, 80 mL soybean-urease solution was introduced to each sand column (from the top) through a peristaltic pump at a rate of 2.0 mL/min according to the research of Choi *et al.* (2017a). It remained for 6 h to ensure an even distribution of urease enzyme within the sand. Then, 80 mL SC or CC was introduced at the same rate (2.0 mL/min), and the sand samples were incubated at room temperature for 18 h. The above biocementation procedure was repeated. Note that it was difficult for the treatment solution to percolate after 6 cycles of treatment. The EICP treatments were stopped after 6 cycles of percolation. After completing the EICP process, all biocemented sand column samples were flushed with 400 mL deionized water to remove the residual unreacted substance and the by-product NH_4Cl in the sand samples. Each set of tests were triplicated for repeatability.

2.5 Properties of biocemented sand columns samples

The biocemented sand column samples were tested to evaluate the physical and mechanical properties, including permeability, unconfined compressive strength (UCS), calcium carbonate content, and sand microstructure.

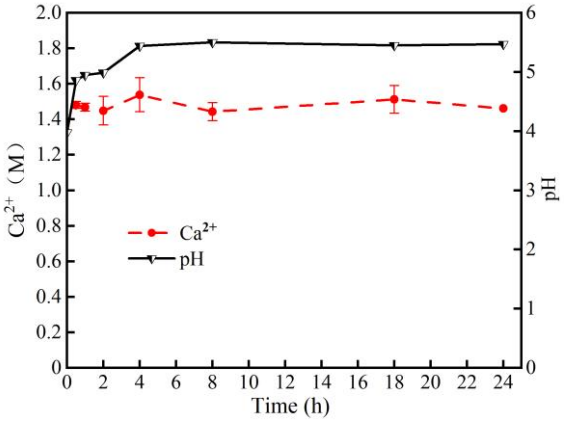

(a) Soluble calcium concentration and pH with acetic acid concentrations

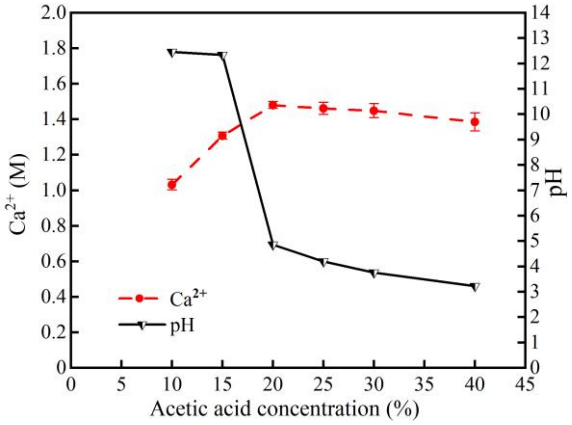

(b) Soluble calcium concentration and pH with time

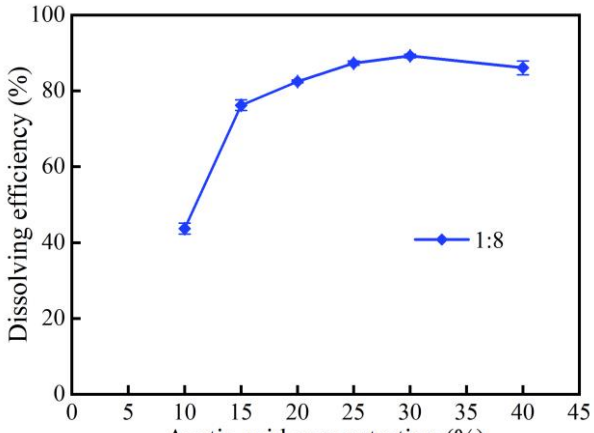

(c) Dissolving efficiency

Fig. 4 Dissolution of CSP in different acetic acid concentrations solutions under solid -to-liquid ratio of 1:8

Permeability tests were carried out using a falling head method (Proto *et al*. 2016). Then, the biocemented sand column samples were oven-dried at 60℃ for 48 h, and the UCS tests were conducted according to the ASTM Standard D2166 (ASTM 2013). After completing the UCS test, sand fragments (~ 5 g each) from the top, middle, and bottom of each sand sample were collected for calcium carbonate content measurement through the acid dissolving method (Cui *et al*. 2020). In this method, the sand fragment was washed with deionized water and then was oven-dried and weighed (M_0). Then, 2 M hydrochloric acid was used to dissolve the $CaCO_3$, and the remaining substance was washed with deionized water, oven-dried, and weighed again (M_1). The calcium carbonate content was calculated as (M_0-M_1)/M_1. The scanning electron microscopy (SEM) and XRD tests were used to analyze the morphological structures of the biocemented sand samples.

3. Results

3.1 Soluble calcium from CSP

Variable-controlling approach was used to explore the effects of acetic acid concentration and solid-to-liquid ratio on the dissolution efficiency of carbide slag. Too low acetic acid concentration or too high solid-to-liquid ratio leads to the insufficient dissolution of carbide slag in acetic acid, and the mixture remains highly alkaline (considering that carbide slag has high alkalinity). When the pH of the solution (a mixture of carbide slag and acetic acid) is below 7, the carbide slag is deemed to be fully dissolved in acetic acid. To optimize the acetic acid concentrations, 25 g CSP was mixed with different concentrations of acetic acid solution (10%, 15%, 20%, 25%, 30%, and 40%) at a fixed solid-to-liquid ratio (w/v) of 1:8. The soluble calcium concentration and pH value of the CSP/acetic acid mixture are shown in Fig. 4. There were not many changes in the soluble calcium concentration and the pH in the mixed solution over time. So the reaction time was set as 30 min in the rest of this work. As is shown in Fig. 4(b), the concentration of soluble calcium increased with increasing the acetic acid concentration. Still, it remained almost stable when the acetic acid concentration reached 20%. Moreover, the pH of the mixture decreased as the acetic acid concentration increased. The pH of the mixture was reduced to less than 7 when 20% acetic acid was used to dissolve the CSP. In Fig. 4(c), the dissolving efficiency of CSP increases with the increase of acetic acid concentration (10%-15%), but it kept nearly constant when the acetic acid

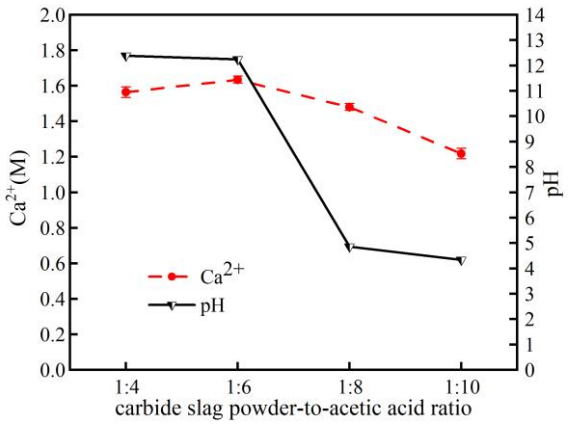

(a) Soluble calcium concentration

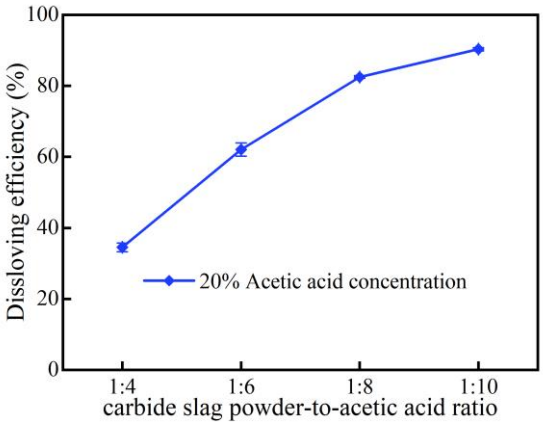

(b) Dissolving efficiency

Fig. 5 Dissolution of CSP in 20% acetic acid concentration solution at various solid -to-liquid ratios

concentration was up to a certain level (>15%). The dissolving efficiency tendency was in good agreement with the soluble calcium concentration (Figs. 4(b)-4(c)).

To optimize the solid-to-liquid ratio (w/v) of CSP to acetic acid, 25 g CSP was mixed with 20% acetic acid solution at different solid-to-liquid ratios, i.e., 1:4, 1:6, 1:8, and 1:10. The soluble calcium concentration and pH value of the CSP/acetic acid mixture are illustrated in Fig. 5. As is shown in Fig. 5(a), the soluble calcium concentration increased first and then decreased with an increase of solid-to-liquid ratio, and the maximum soluble calcium concentration was obtained at a solid-to-liquid ratio of 1:6. However, the CSP/acetic acid mixture was still in a highly alkaline state at a solid-to-liquid ratio of 1:6, indicating that there was still a large amount of $Ca(OH)_2$ need to be neutralized. As shown in Fig. 5(b), the dissolving efficiency of CSP was only 63% at the solid-to-liquid ratio of 1:6, verifying the validity of the above conclusion. From the aspect of soluble calcium concentration, dissolving efficiency, and cost, 20% acetic acid was used to produce the soluble calcium and the solid-to-liquid ratio was fixed at 1:8 hereafter. Under these conditions, the concentration of soluble calcium was about 1.5 M.

3.2 Confirmation of EICP process in soil-free solution

Fig. 6 presents the variation of calcium concentration with time for the EICP solution (including soybean-urease, urea, and soluble calcium or reagent grade $CaCl_2$) at an initial calcium concentration of 0.25 M. The consumption of calcium ion provided a systematic way to estimate the precipitation mass and precipitation ratio in EICP. For both SC and CC, the calcium concentration of the solution gradually decreased with time, approximately reaching a minimum value within 12 hours and remained constant afterward. However, more calcium took part in the biochemical reaction when reagent grade $CaCl_2$ was employed as the calcium source, compared to soluble calcium. The XRD analysis of the precipitated substances in soil-free solution tests is shown in Fig. 7. The XRD results were compared with typical diffraction spectra of $CaCO_3$

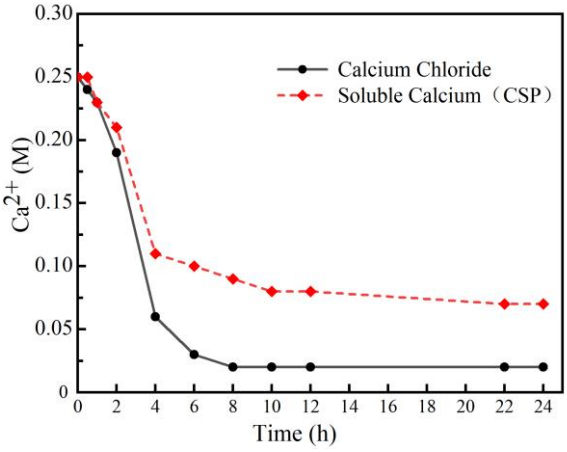

Fig. 6 The changes in calcium concentration with time in soil-free solution

(calcite and vaterite). The results confirmed that the precipitate was $CaCO_3$, and validated the feasibility of using CSP-derived soluble calcium to produce $CaCO_3$ in the EICP process. The quantification of relative abundances of the calcite and vaterite was undertaken further by comparing the integral area of the major characteristic peaks with measured ratios in a baseline sample of known composition. The type of $CaCO_3$ precipitated by the SC was different from that precipitated by the CC. 95% vaterite and 5% calcite precipitated when SC was used in the EICP process, whereas the precipitate was mainly calcite (82%) as CC was used.

3.3 Soil improvement via EICP-based biocementation

3.3.1 Calcium carbonate content and permeability

The calcium carbonate content and permeability of different sand columns are shown in Table 1. The calcium carbonate content ranged from 3.8% to 4.4% for the biocemented sand columns, and the two types of calcium sources (soluble calcium and reagent grade $CaCl_2$) gave

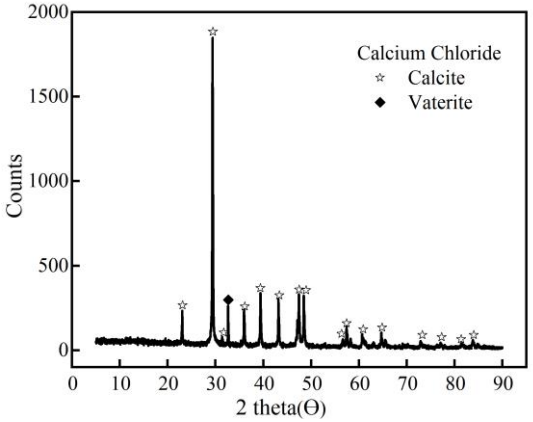

(a) Reagent grade $CaCl_2$ as the calcium salt

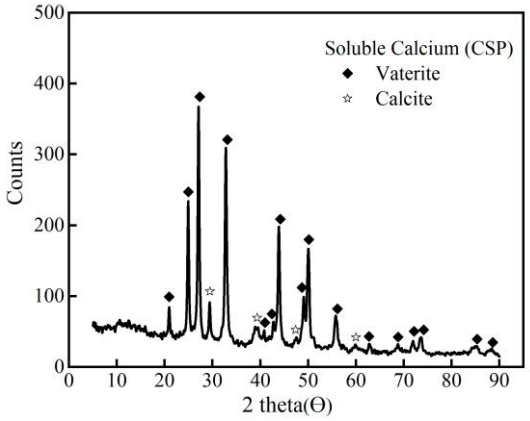

(b) Soluble calcium as the calcium salt

Fig. 7 The XRD patterns of the precipitated substances in soil-free solution

Table 1 The calcium carbonate content and permeability of different biocemented sand columns

Sample No.	Calcium source	Permeability (10^{-6}m/s)	Calcium Carbonate Content(%)			
			Top	Middle	Bottom	Average
CC-1	Reagent grade $CaCl_2$	8.45	3.0	3.5	5.1	3.8
CC-2		5.47	3.4	4.0	5.0	4.1
CC-3		4.39	5.8	3.3	4.2	4.4
SC-1	Soluble calcium	5.38	3.6	3.8	5.1	4.2
SC-2		7.31	3.2	3.8	5.0	4.0
SC-3		8.78	3.1	4.6	3.6	3.8

statistically similar results ($p>0.05$) in terms of calcium carbonate production. The calcium carbonate content of biocemented sand columns increased from the top to the bottom except for a few samples. The results of this study confirmed the uneven distribution of calcium carbonate in the biocemented sand column caused by the two-phase injection method (Cui *et al*. 2020).

Fig. 8 shows the relationship between permeability and calcium carbonate content of biocemented sand. The permeability reduced from 1.27×10^{-4} m/s for the untreated sand to $8.78\text{-}4.39\times10^{-6}$ m/s for the EICP treated sand. In addition, the permeability of the biocemented sand column reached the same order of magnitude for similar calcium carbonate content, whichever calcium source was used to produce the biological $CaCO_3$. Similar phenomena were reported by Cheng *et al*. (2017) and Choi *et al*. (2017a) that the permeability of biocementation treated sand decreased with the $CaCO_3$ content.

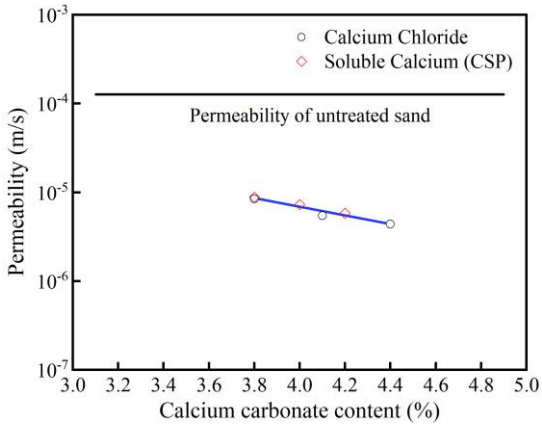

Fig. 8 The relationship between permeability and calcium carbonate content of biocemented sand

3.3.2 Unconfined compressive strength

Fig. 9 shows the stress-strain behavior of biocemented sand obtained through the UCS tests. All the EICP-treated sand samples exhibited a brittle nature comparable to those observed in MICP (Choi *et al*. 2017a) and EICP (Kavazanjian and Hamdan 2015) treatment. Based on the data in Fig. 9 and Table 1, the UCS values of biocemented sand samples are plotted as a function of calcium carbonate content shown in Fig. 10. For all biocemented sand samples, the UCS value increased with the increase of the calcium carbonate content, which was in line with previous results (Yasuhara *et al.* 2012, Kavazanjian and Hamdan 2015, Hamed *et al*. 2018). The UCS and calcium carbonate content trend line was also fitted with high correlation coefficients (R^2=0.906) within the calcium carbonate content range of 3.8%-4.4%.

3.3.3 SEM and XRD analyses of EICP treated sand columns

The microstructure of the biocemented sand samples was investigated by SEM (Fig. 11). It can be seen from

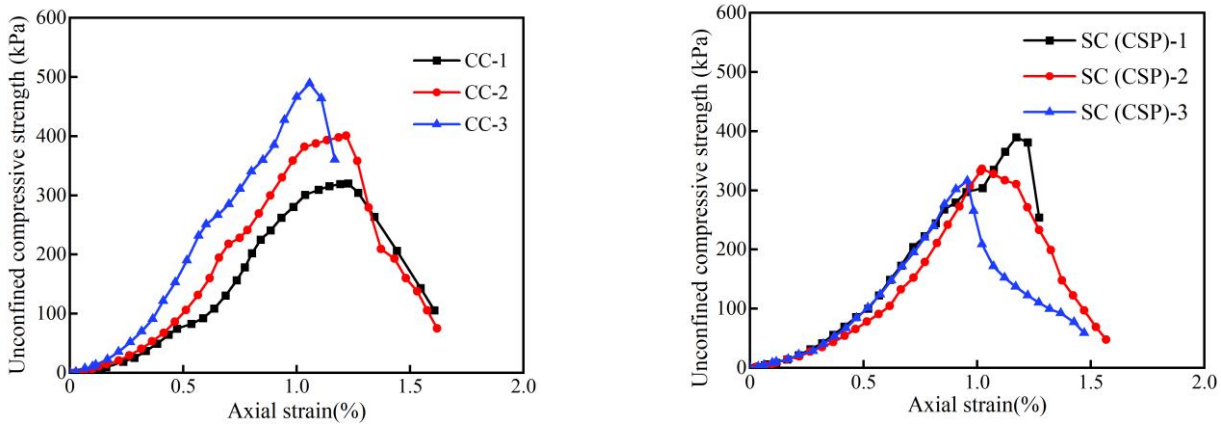

(a) Reagent grade $CaCl_2$ as the calcium salt (b) Soluble calcium as the calcium salt

Fig. 9 The unconfined compressive stress-axial strain relationship of biocemented sand

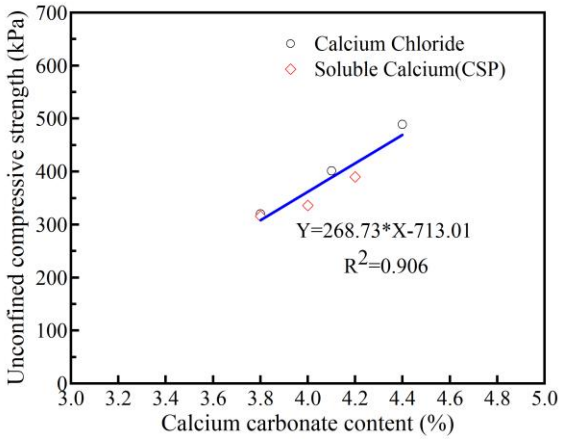

Fig. 10 The correlation between calcium carbonate content and UCS

Figs. 11(a), 11(b), 11(d), and 11(e) that spherical crystals appeared both at particle contacts and on particle surfaces of the EICP-treated sand, filling the sand pores and coating the sand particles. However, as is shown in Figs. 11(c) and 11(f), the surface of spherical crystal on the sand sample treated with soluble calcium as the calcium salt had a filiform texture, while it was not observed in the sand sample treated with CC. XRD analysis (Fig. 12) showed that quartz and calcite existed in the CC-based biocemented sand, while quartz and vaterite were observed in the SC-based biocemented sand. This was consistent with the XRD results of the precipitated substances in soil-free solution (Fig. 7).

4. Discussions

Plant-derived urease-induced calcium carbonate precipitation has some advantages over the commonly used MICP process for soil improvement. The plant-derived urease method is free from issues related to the complex cultivation process of bacteria and bio-safety. In addition, the smaller size of free urease, compared to the bacterial cell, facilitates the application of free urease in finer soil such as silt and clay. However, the large-scale application of plant-derived urease-induced calcium carbonate precipitation may be limited by its high cost at this stage. For one thing, the cost of commercially available urease enzyme comprises 57%–98% of the total cost of the biocementation (Almajed *et al*. 2018). For another, the biocementation process usually requires a large amount of $CaCl_2$ to produce adequate calcium carbonate crystals in soil; the production of $CaCl_2$ is energy-intensive and environmentally unfriendly. In this study, considering the current price of soybeans, the material cost of the crude soybean-urease (soybean powder concentration: 40 g/L) was about US\$0.024 L^{-1}, which was much lower than that of the commonly used *Sporosarcina pasteurii* and purified urease enzyme. In addition, producing calcium ions from carbide slag is an environmentally friendly method for waste recycling and biocementation process. Additionally, producing $CaCO_3$ via waste-derived-calcium reduces the adverse effects of chloride ions on natural plants and corrosion of the steel reinforcement in construction engineering (Yuan *et al.* 2009). As a solid waste produced in large quantities in the chemical industry, carbide slag causes a series of environmental problems such as land salinization

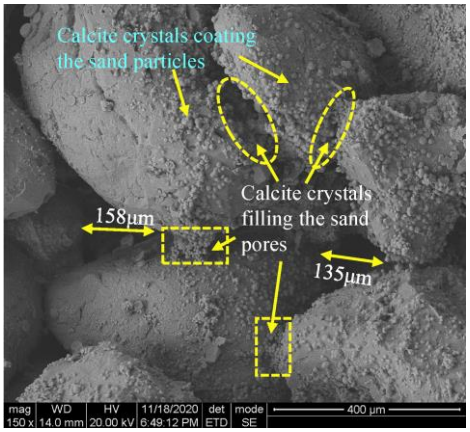

(a) Reagent grade $CaCl_2$ as the calcium salt magnification factor ×150

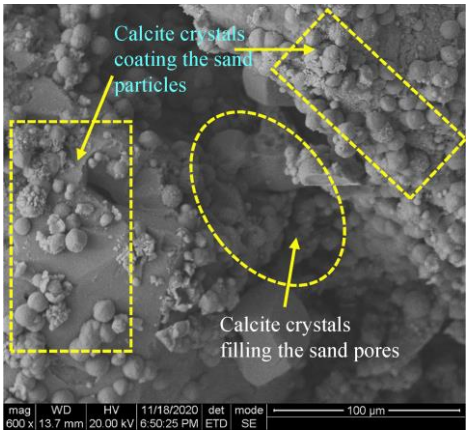

(b) Reagent grade $CaCl_2$ as the calcium salt magnification factor ×600

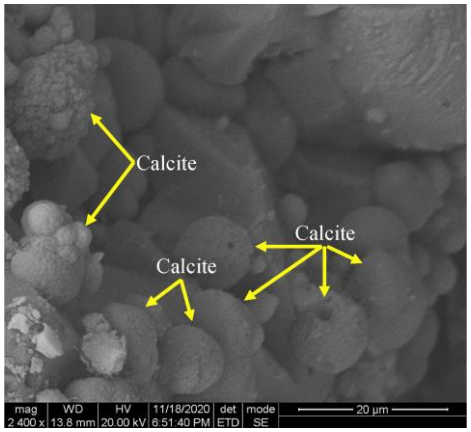

(c) Reagent grade $CaCl_2$ as the calcium salt magnification factor ×2400

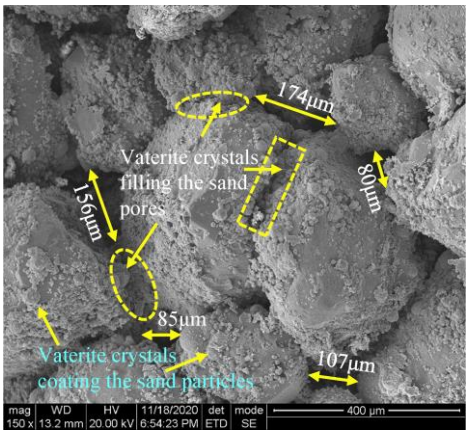

(d) Soluble calcium as the calcium salt magnification factors ×150

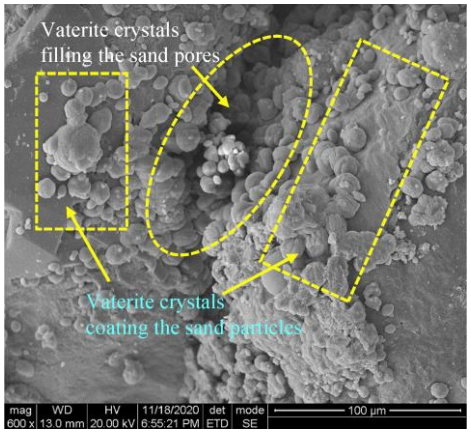

(e) Soluble calcium as the calcium salt magnification factors ×600

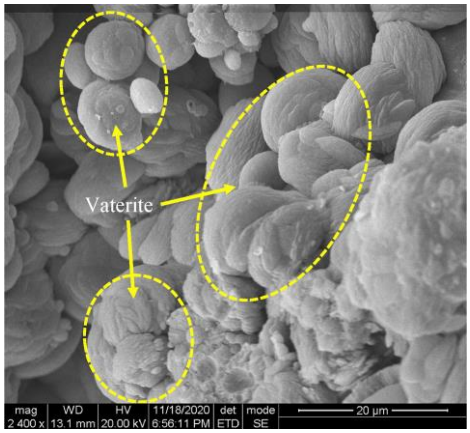

(f) Soluble calcium as the calcium salt magnification factors ×2400

Fig. 11 The SEM images of biocemented sand columns with different magnification

and water pollution. Making full use of calcium in carbide slag not only reduces the damage it made to the environment but also achieves the resource utilization of waste, which is in line with the development trend of the green chemical industry. This study confirmed the feasibility of producing soluble calcium from industrial solid waste CSP and its application in EICP-based biocementation. Acetic acid was employed to extract soluble calcium from CSP in this work. It can be seen from Figs. 4(a) and 4(c) that the concentration of soluble calcium did not significantly increase as the acetic acid concentration exceeded 20%. The dissolving efficiency of CSP decreased slightly at the acetic acid concentration of 40%. This was somewhat different from the results gained by other researchers who used calcareous sand and acetic acid to produce soluble calcium (Liu *et al.* 2018). This

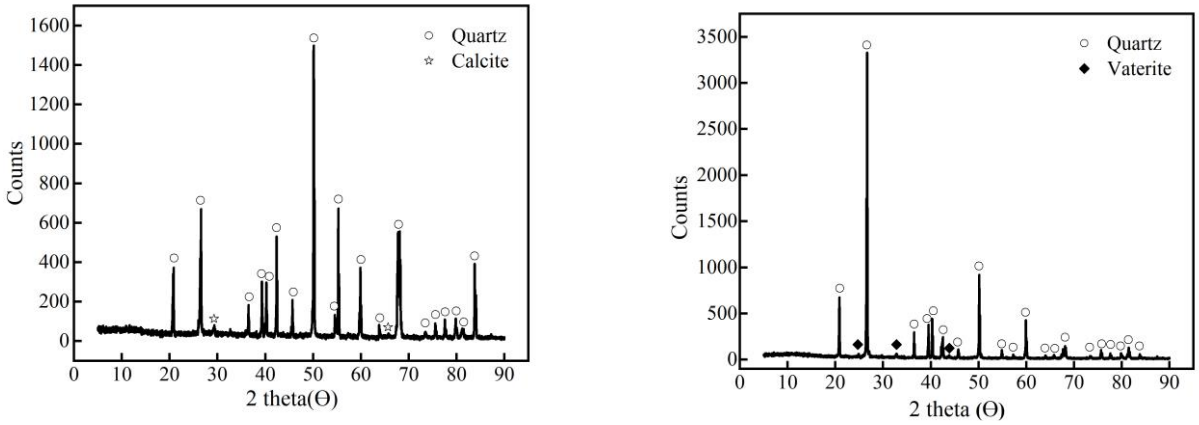

(a) Reagent grade $CaCl_2$ (b) Soluble calcium

Fig. 12 The XRD patterns of biocemented sand columns using different calcium salts

phenomenon might be related to excessive acetic acid concentration. It was also worth noting that the human factors in the experiment process cannot be ignored, bringing about a certain deviation. Considering the effect of acetic acid and CSP amount on extracting soluble calcium and the cost (mainly refers to the acetic acid), it is unnecessary to use acetic acid with a higher than 20% concentration. In this work, 20% acetic acid and a solid (CSP)-to-liquid (20% acetic acid) ratio of 1:8 were recommended to produce soluble calcium from CSP. At the above condition, the concentration of soluble calcium could reach 1.5 M, which is sufficient for bio-catalyzed $CaCO_3$ precipitation. In addition, it should be noted that carbide slag is a heterogeneous material, and there are certain differences in the calcium content in the waste carbide slag produced from different regions and different calcium carbides. In practice, the appropriate acetic acid concentration and solid-to-liquid ratio should be decided according to the actual situation.

The physical and mechanical properties of the EICP treated sand columns using CSP-derived soluble calcium were investigated. Compared to the reagent grade $CaCl_2$, EICP treatment using CSP-derived soluble calcium as the calcium salt brought about similar calcium carbonate content, the same degree of permeability reduction, but a slightly lower UCS value of sand. Other researchers report that the UCS values of biocemented sand columns treated with calcium acetate are higher than those treated with reagent grade $CaCl_2$, which is contrary to the results of this research (Zhang *et al.* 2014, Zhang *et al*. 2015, Choi *et al.* 2016, Liu *et al*. 2018). Some reasons may account for this difference. As shown in Figs. 7 and 12, calcite was the primary crystal type in the $CaCl_2$-based biocemented sand, while vaterite was dominant in the soluble calcium (mainly calcium acetate)-based biocemented sand. Calcite is a more stable polymorph of calcium carbonate and likely possesses a higher binding strength in the clusters than other types (Gebauer *et al.* 2008). In addition, the surface of spherical vaterite crystal precipitated in the soluble calcium-based biocemented sand is much smoother, which may have an adverse influence on the strength. The effect of crystal morphology of calcium carbonate on the strength of biocemented sand was also recognized by (Cui *et al.* 2020). The difference type of $CaCO_3$ crystals might be related to calcium sources and other ions in the soluble calcium solution. For example, Zhang *et al*. (2014) found that the crystal type of the MICP-treated samples using calcium acetate is mainly aragonite, while that using $CaCl_2$ or $Ca(NO_3)_2$ is mainly calcite. Putra *et al.* (2016) added magnesium chloride into EICP solution (composed of urea, urease and calcium) and found that aragonite is formed. Based on the XRF results, the CSP contains magnesium, which may account for the presence of vaterite in the soluble calcium (mainly calcium acetate)-based biocemented sand. Further study is needed to investigate the factors affecting the formation of $CaCO_3$ morphology in different EICP processes. It should be noted that the average UCS value of soluble calcium-based biocemented sand samples reaches 350 kPa, demonstrating that soluble calcium produced from CSP can be used as the calcium source for the EICP process to improve the mechanical properties of sand.

Moreover, at the same level of calcium carbonate content, the UCS values of EICP treated sand samples were higher than those of MICP treated sand samples comparing with others research (Cheng *et al*. 2013, Qabany and Soga 2013, Choi *et al.* 2016). The results agreed with previous results reported by Hoang *et al*. (2020) and Nafisi *et al.* (2019) and indicated that the EICP method had a certain superiority over the MICP method in soil improvement. However, it should be noted that the current biocementation method also some challenges, such as the use of commercial acetic acid to dissolve the CSP, emission of ammonia due to urea hydrolysis, and the energy-intensive process required during the production of urea. In addition, many factors such as product inhibition, urease inhibition, pH, temperature, etc, would affect the kinetic of the overall precipitation reaction of soybeans-urease induced carbonate precipitation. Further investigation is necessary to find out an economical soybean powder concentration and an optimized reaction conditions for soybeans-urease induced carbonate precipitation. Much more efforts need to be made to address the practical problems mentioned above, which is critical for the large-scale application of EICP.

5. Conclusions

This study proposed a method to produce soluble calcium using CSP and investigated the performance of EICP-based biocementation in soil improvement. The following conclusions could be drawn:

- A new soluble calcium source was obtained by the use of CSP and acetic acid. After conditions were optimized, the maximum concentration of calcium ion reached at 1.5 M, which was sufficient for biocementation.
- After being treated with soluble calcium, the permeability reduced from an order of magnitude 10^{-4} to 10^{-6} and the UCS value increased from 0 to 350 kPa at a calcium carbonate content of about 4%. Compared to the reagent grade $CaCl_2$, EICP treatment of sand using CSP-derived soluble calcium as the calcium salt brought back a similar calcium carbonate content, the same degree of permeability reduction, but a slightly lower UCS value.
- SEM and XRD analyses revealed that spherical calcium carbonate crystals precipitated both at particle contacts and on particle surfaces of the EICP-treated sand. These crystals were mainly vaterite when the soluble calcium was used.

Acknowledgments

The research presented in this paper was financially supported by Natural Science Foundation of China (Projects No. 51978244, 51979088, and 52078188).

References

Achal, V., Mukherjee, A. and Reddy, M. S. (2010), "ORIGINAL RESEARCH: Biocalcification by Sporosarcina pasteurii using corn steep liquor as the nutrient source", *Ind. Biotechnol.*, **6**(3), 170-174. https://doi.org/10.1089/ind.2010.6.170.

Al Imran, M., Nakashima, K., Evelpidou, N. and Kawasaki, S. (2019), "Factors affecting the urease activity of native ureolytic bacteria isolated from coastal areas", *Geomech. Eng.*, **17**(5), 421-427. https://doi.org/10.12989/gae.2019.17.5.421.

Almajed, A., Tirkolaei, H.K. and Kavazanjian, E. (2018), "Baseline investigation on enzyme-induced calcium carbonate precipitation", *J. Geotech. Geoenviron. Eng.*, **144**(11), https://doi.org/10.1061/(ASCE)GT.1943-5606.0001973.

Almajed, A., Tirkolaei, H.K., Kavazanjian, E. and Hamdan, N. (2019), "Enzyme induced biocementated sand with high strength at low carbonate content", *Sci. Rep.*, **9**(1). https://doi.org/10.1038/s41598-018-38361-1.

ASTM. (2012), "*Standard Specification for Standard Sand*", ASTM C778-12, ASTM International, West Conshohocken, PA.

ASTM. (2013), "*Standard Test Method for Unconfined Compressive Strength of Cohesive Soil*" , ASTM D2166, ASTM International, West Conshohocken, PA.

Cheng, L., Cord-Ruwisch, R. and Shahin, M.A. (2013), "Cementation of sand soil by microbially induced calcite precipitation at various degrees of saturation", *Can. Geotech. J.*, **50**(1), 81-90. https://doi.org/10.1139/cgj-2012-0023.

Cheng, L., Shahin, M.A. and Cord-Ruwisch, R. (2014), "Bio-cementation of sandy soil using microbially induced carbonate precipitation for marine environments", *Geotechnique*, **64**(12), 1010-1013. https://doi.org/10.1680/geot.14.T.025.

Cheng, L., Shahin, M.A. and Mujah, D. (2017), "Influence of key environmental conditions on microbially induced cementation for soil stabilization", *J. Geotech. Geoenviron. Eng.*, **143**(1), https://doi.org/10.1061/(ASCE)GT.1943-5606.0001586.

Choi, S.G., Chu, J., and Kwon, T.H. (2019), "Effect of chemical concentrations on strength and crystal size of biocemented sand", *Geomechanics and Engineering*, **17**(5), 465-473. https://doi.org/10.12989/gae.2019.17.5.465.

Choi, S.G., Chu, J., Brown, R.C., Wang, K. and Wen, Z. (2017a), "Sustainable biocement production via microbially induced calcium carbonate precipitation: Use of limestone and acetic acid derived from pyrolysis of lignocellulosic biomass", *ACS Sust. Chem. Eng.*, **5**(6), 5183-5190. https://doi.org/10.1021/acssuschemeng.7b00521.

Choi, S.G., Park, S.S., Wu, S.F. and Chu, J. (2017b), "Methods for calcium carbonate content measurement of biocemented soils", *J. Mater. Civil Eng.*, **29**(11). https://doi.org/10.1061/(ASCE)MT.1943-5533.0002064.

Choi, S.G., Wu, S.F. and Chu, J. (2016), "Biocementation for Sand Using an Eggshell as Calcium Source", *J. Geotech. Geoenviron. Eng.*, **142**(10). https://doi.org/10.1061/(ASCE)GT.1943-5606.0001534.

Chu, J., Stabnikov, V. and Ivanov, V. (2012), "Microbially induced calcium carbonate precipitation on surface or in the bulk of soil", *Geomicrobio. J.*, **29**(6), 544-549. https://doi.org/10.1080/01490451.2011.592929.

Chung, J.S., Kim, B.H. and Kim, I.S. (2014), "A case study on chloride corrosion for the end zone of concrete deck subjected to de-icing salts added calcium chloride", *J. Korean Soc. Saf.*, **29**(6),87-93. https://doi.org/10.14346/JKOSOS.2014.29.6.087.

Cuccurullo, A., Gallipoli, D., Bruno, A.W., Augarde, C. and Borderie, C.L. (2020), "Earth stabilisation via carbonate precipitation by plant-derived urease for building applications", *Geomech. Energy Environ.*, (5), 100230. https://doi.org/10.1016/j.gete.2020.100230.

Cui, M.J., Lai, H.J., Hoang, T. and Chu, J. (2020), "One-phase-low-pH enzyme induced carbonate precipitation (EICP) method for soil improvement", Acta Geotechnica, **16**(2), 481-489. https://doi.org/10.1007/s11440-020-01043-2.

Dilrukshi, R.A.N., Nakashima, K. and Kawasaki, S. (2018), "Soil improvement using plant-derived urease-induced calcium carbonate precipitation", *Soils Found.*, **58**(4), 894-910. https://doi.org/10.1016/j.sandf.2018.04.003.

Do, J., Montoya, B.M. and Gabr, M.A. (2019), "Debonding of microbially induced carbonate precipitation-stabilized sand by shearing and erosion", *Geomech. Eng.*, **17**(5), 429-438. https://doi.org/10.12989/gae.2019.17.5.429.

Gao, Y., He, J., Tang, X. and Chu, J. (2019), "Calcium carbonate precipitation catalyzed by soybean urease as an improvement method for fine-grained soil", *Soils Found.*, **59**(5), 1631-1637. https://doi.org/10.1016/j.sandf.2019.03.014.

Gebauer, D., Volkel, A. and Colfen, H. (2008), "Stable prenucleation calcium carbonate clusters", *Science*, **322**(5909), 1819-1822. https://doi.org/10.1126/science.1164271.

Hamdan, N. and Kavazanjian, E. (2016), "Enzyme-induced carbonate mineral precipitation for fugitive dust control", *Géotechnique*, **66**(7), 546-555. https://doi.org/10.1680/jgeot.15.P.168.

Hamed, K.T., Martin, K., Krishnan, V. and Kavazanjian, E. (2018), "Bench-scale bio-grouted column formation using enzyme-induced carbonate precipitation", *B2G,* Atlanta,USA, October.

Hang, L., Gao, Y., He, J. and Chu, J. (2019), "Mechanical behaviour of biocemented sand under triaxial consolidated undrained or constant shear drained conditions", *Geomech. Eng.*, **17**(5), 497-505. https://doi.org/10.12989/gae.2019.17.5.497.

He, J., Gao, Y., Gu, Z., Chu, J. and Wang, L. (2020), "Characterization of crude bacterial urease for $CaCO_3$

precipitation and cementation of silty sand", *J. Mater. Civil Eng.*, **32**(5), 04020071.04020071-04020071.04020079. https://doi.org/10.1061/(ASCE)MT.1943-5533.0003100.

Hoang, T., Alleman, J., Cetin, B. and Choi, S.G. (2020), "Engineering properties of biocementation coarse- and fine-grained sand catalyzed by bacterial cells and bacterial enzyme", *J. Mater. Civil Eng.*, **32**(4), https://doi.org/10.1061/(ASCE)MT.1943-5533.0003083.

Hoang, T., Alleman, J., Cetin, B., Ikuma, K. and Choi, S.G. (2019), "Sand and silty-sand soil stabilization using bacterial enzyme-induced calcite precipitation (BEICP)", *Can. Geotech. J.*, **56**(6), 808-822. https://doi.org/10.1139/cgj-2018-0191.

Javadi, N., Khodadadi, H., Hamdan, N. and Kavazanjian, E. (2018), "EICP Treatment of Soil by Using Urease Enzyme Extracted from Watermelon Seeds", *Proceedings of the IFCEE 2018*, 115-124.

Junjie, F., Deguang, C., Zhenzi, J., Yi, Z., Li, P.U. and Yani, J. (2014), "Synthesis and microstructure analysis of autoclaved aerated concrete with carbide slag addition", *J. Wuhan Univ. Technol.*, **29**(5),1005-1010. https://doi.org/ 10.1007/s11595-014-1034-0.

Kavazanjian, E. and Hamdan, N. (2015), "Enzyme Induced Carbonate Precipitation (EICP) columns for ground improvement", *Geo-congress*.

Khodadadi, T.H., Kavazanjian, E., van Paassen, L. and DeJong, J. (2017), "Bio-grout materials: A review", *Proceedings of the 5th International Conference on Grouting, Deep Mixing, and Diaphragm Walls*, 1-12. https://doi.org/10.1061/9780784480793.001.

Li, W., Yi, Y. and Puppala, A.J. (2019), "Utilization of carbide slag-activated ground granulated blastfurnace slag to treat gypseous soil", *Soils Found.*, **59**(5), 1496-1507. https://doi.org/10.1016/j.sandf.2019.06.002.

Liang, S., Chen, J., Niu, J., Gong, X. and Feng, D. (2019), "Using recycled calcium sources to solidify sandy soil through microbial induced carbonate precipitation", *Mar. Georesour. Geotechnol.*, **38**(4), 393-399. https://doi.org/10.1080/1064119x.2019.1575939.

Liu, L., Liu, H., Xiao, Y., Chu, J., Xiao, P. and Wang, Y. (2018), "Biocementation of calcareous sand using soluble calcium derived from calcareous sand", *Bull. Eng. Geol. Environ.*, **77**(4), 1781-1791. https://doi.org/10.1007/s10064-017-1106-4.

Martinez, B.C., DeJong, J.T., Ginn, T.R., Montoya, B.M., Barkouki, T.H., Hunt, C., Tanyu, B. and Major, D. (2013), "Experimental optimization of microbial-induced carbonate precipitation for soil improvement", *J. Geotech. Geoenviron. Eng.*, **139**(4), 587-598. https://doi.org/10.1061/(ASCE)GT.1943-5606.0000787.

Meng, H., Gao, Y., He, J., Qi, Y. and Hang, L. (2021a), "Microbially induced carbonate precipitation for wind erosion control of desert soil: Field-scale tests", *Geoderma*, **383.** https://doi.org/10.1016/j.geoderma.2020.114723.

Meng, H., Shu, S., Gao, Y., Yan, B. and He, J. (2021b), "Multiple-phase enzyme-induced carbonate precipitation (EICP) method for soil improvement", *Eng. Geol.*, **294**(11), 106374. https://10.1016/j.enggeo.2021.106374.

Montoya, B.M. and DeJong, J.T. (2015), "Stress-strain behavior of sands cemented by microbially induced calcite precipitation", *J. Geotech. Geoenviron. Eng.*, **141**(6). https://doi.org/10.1061/(ASCE)GT.1943-5606.0001302.

Nafisi, A., Safavizadeh, S. and Montoya, B.M. (2019), "Influence of microbe and enzyme-induced treatments on cemented sand shear response", *J. Geotech. Geoenviron. Eng.*, **145**(9). https://doi.org/10.1061/(ASCE)GT.1943-5606.0002111.

Nam, I.H., Chon, C.M., Jung, K.Y., Choi, S.G., Choi, H. and Park, S.S. (2014), "Calcite precipitation by ureolytic plant (Canavalia ensiformis) extracts as effective biomaterials", *KSCE J. Civil Eng.*, **19**(6), 1620-1625. https://doi.org/ 10.1007/s12205-014-0558-3.

Paassen, L.A.V., Ghose, R., Linden, T.J.M.V.D., Star, W.R.L.V.D. and Loosdrecht, M.C.M.V. (2010), "Quantifying biomediated ground improvement by ureolysis: Large-scale biogrout experiment", *J. Geotech. Geoenviron. Eng.*, **136**(12), 1721-1728. https://doi.org/10.1061/(ASCE)GT.1943-5606.0000382.

Park, S.S., Choi, S.G. and Nam, I.H. (2014), "Effect of plant-induced calcite precipitation on the strength of sand", *J. Mater. Civil Eng.*, **26**(8). https://doi.org/10.1061/(ASCE)MT.1943-5533.0001029.

Phua, Y.J. and Royne, A. (2018), "Bio-cementation through controlled dissolution and recrystallization of calcium carbonate", *Constr. Build. Mater.*, **16,** 7657-668. https://doi.org/10.1016/j.conbuildmat.2018.02.059.

Proto, C.J., DeJong, J.T. and Nelson, D.C. (2016), "Biomediated permeability reduction of saturated sands", *J. Geotech. Geoenviron. Eng.*, **142**(12). https://doi.org/10.1061/(ASCE)GT.1943-5606.0001558.

Putra, H., Yasuhara, H., Kinoshita, N., Neupane, D. and Lu, C.W. (2016), "Effect of magnesium as substitute material in enzyme-mediated calcite precipitation for soil-improvement technique", *Front. Bioeng. Biotechnol.*, **4**(37). https://doi.org/10.3389/fbioe.2016.00037.

Qabany, A.A. and Soga, K. (2013), "Effect of chemical treatment used in MICP on engineering properties of cemented soils", *Géotechnique*, **63**(4), 331-339. https://doi.org/10.1680/geot.SIP13.P.022.

Ran, D. and Kawasaki, S. (2016), "Effective use of plant-derived urease in the field of geoenvironmental/ geotechnical engineering", *J. Civil Environ. Eng.*, **6**(1). https://doi.org/10.4172/2165-784x.1000207.

Sidik, W.S., Canakci, H., Kilic, I.H. and Celik, F. (2014), "Applicability of biocementation for organic soil and its effect on permeability", *Geomech. Eng.*, **7**(6), 649-663. https://doi.org/10.12989/gae.2014.7.6.649.

Song, J.Y., Sim, Y., Yeom, S., Jang, J. and Yun, T.S. (2020), "Stiffness loss in enzyme-induced carbonate precipitated sand with stress scenarios", *Geomech. Eng.*, **20**(2), 165-174. https://doi.org/10.12989/gae.2020.20.2.165.

Tao, X., Zhang, G., Zhang, P., Wang, S., Nabi, M. and Wang, H. (2018), "Thermo-carbide slag pretreatment of energy plants for enhancing enzymatic hydrolysis", *Ind. Crops Products*, **120,** 77-83. https://doi.org/10.1016/j.indcrop.2018.04.038.

Tirkolaei, H.K., Javadi, N., Krishnan, V., Hamdan, N. and Kavazanjian, E. (2020), "Crude urease extract for biocementation", *J. Mater. Civil Eng.*, **32**(12). https://doi.org/10.1061/(ASCE)MT.1943-5533.0003466.

Wang, Y., Ye, B., Hong, Z., Wang, Y. and Liu, M. (2020), "Uniform calcite mircro/nanorods preparation from carbide slag using recyclable citrate extractant", *J. Cleaner Production*, **253**. https://doi.org/10.1016/j.jclepro.2019.119930.

Whiffin, V.S., van Paassen, L.A. and Harkes, M.P. (2007), "Microbial carbonate precipitation as a soil improvement technique", *Geomicrobio. J.*, **24**(5),417-423. https://doi.org/10.1080/01490450701436505.

Yasuhara, H., Neupane, D., Hayashi, K. and Okamura, M. (2012), "Experiments and predictions of physical properties of sand cemented by enzymatically-induced carbonate precipitation", *Soils Found.*, **52**(3), 539-549. https://doi.org/10.1016/j.sandf.2012.05.011.

Yuan, Q., Shi, C., Schutter, G.D., Audenaert, K. and Deng, D. (2009), "Chloride binding of cement-based materials subjected to external chloride environment – A review", *Constr. Build. Mater.*, **23**(1), 1-13. https://doi.org/10.1016/j.conbuildmat.2008.02.004.

Zhang, Y., Guo, H.X. and Cheng, X.H. (2014), "Influences of

calcium sources on microbially induced carbonate precipitation in porous media", *Mater. Res. Innov.*, **18**(2), 79-84. https://doi.org/10.1179/1432891714z.000000000384.

Zhang, Y., Guo, H.X. and Cheng, X.H. (2015), "Role of calcium sources in the strength and microstructure of microbial mortar", *Constr. Build. Mater.*, **77**. 160-167. https://doi.org/10.1016/j.conbuildmat.2014.12.040.

IC